Computation of X-Ray Photoelectron Spectroscopy via a Real-time Cumulant Approach

Jonathan Curtis,[1] Joshua Kas,[2] Fernando Vila,[2] and John Rehr[2]
[1] *Department of Physics, University of Rochester, Rochester, NY 14927*
[2] *Department of Physics, University of Washington, Seattle, WA 98195*
(Dated: September 2, 2015)

Via a real-time, cumulant based approach, the X-Ray Photoelectron Spectrum (XPS) for molecular C_{60} Buckminsterfullerene, Nickel, Iron, and Cobalt are computed. Good agreement with experiment is found in the case of C_{60}. We also use this approach to compute quasi-particle peak shifts and weights. We find that in the case of the transition metals, the analytic calculation appears to be an overestimate of satellite weight when compared to direct integration of the spectral functions.

I. INTRODUCTION

The field of X-Ray spectroscopy, and in particular, the technique of X-Ray Photoelectron Spectroscopy (XPS) has seen widespread success in its application to problems in nano-science, materials science, chemistry, and condensed matter physics. Of particular importance to these fields is the ability to accurately and efficiently compute theoretically predicted spectra, against which experimentally measured spectra may be compared. XPS, as an experimental technique, allows one to perform an in-depth analysis of the many-body physics involved in the excitations of a sample. Since the physics that underlies these many-body interactions is inherently complex, computing X-Ray spectra, and in particular, XPS, is often a matter of choosing appropriate approximation techniques and approaches. For instance, though the well-known "GW" approximation (GWA) of Hedin [2, 3] is useful for studying the main quasi-particle features of many systems, as was pointed out in [1], the standard GWA often fails to correctly predict the structure of the satellite spectra in photoelectric emission processes. To remedy this, a new approach, based on a function known as "the cumulant" was employed [6, 8]. This approach has since been employed successfully in many instances [1, 4, 6] and has been used to predict both main quasi-particle features as well as satellite structures. In this this project, a cumulant based approach was used to study the photoelectric emission spectrum for C_{60} fullerene in the gas phase as well as the transition metals Fe, Ni, and Co in their metallic (crystalline) phases.

A. Fullerene

Buckminsterfullerene, henceforth referred to simply as "C_{60}," is an allotrope of Carbon (atomic number 6) comprised of 60 atoms bonded into a truncated icosahedron resembling a soccer ball [5]. Though C_{60} was only discovered recently (1985), this molecule, and the related family of "fullerene" allotropes have already been examined extensively due to the variety of remarkable properties they have been shown to exhibit. C_{60} can exist in both a gaseous phase, and in a solid phase (fullerite), in which it forms a face centered cubic (fcc) crystalline structure that is naturally an n-type semiconductor. Seeing as collective excitations such as plasmons, polarons, and phonons play a crucial role in the behavior of such materials, it is important to understand the nature of many-body effects in fullerite. Though it would be ideal to study the case of crystalline fullerite, such as system would consist of of upwards of $\sim 60 \times 8 \approx 480$ atoms per unit cell. Thus, due to computational limitations we have restricted our study to C_{60} in the gaseous phase as a proxy for the case of fullerite. This approximation will be justified *post-hoc* via comparison with experiment.

B. Transition Metals

Whereas C_{60} may present itself as a fallaciously complex system to study, transition metals provide the opposite. Broadly speaking, transition metals are elements that have a valence shell comprised of electrons in the 3d orbitals (though this usage of orbitals becomes questionable for elements with atomic number this large). Despite their often simplistic crystalline structures and metallic bonding mechanisms, strongly-correlated states and non-trivial band structures can lead to complex and interesting many-body effects in transition metal systems [10]. Furthermore, due to their widely varying chemical, electromagnetic, and spectral properties, the study of transition metals from first-principles calculations is important to a variety of fields. Specifically, we will focus on pure metal systems of elements Iron (atomic number 26), Cobalt (atomic number 27), and Nickel (atomic number 28). Our main focus is on the plasmon structures of these metals, where will show that the satellite and main quasi-particle structures are nearly inseparable, indicating the presence of satellite excitations with very little to no gap above the main quasi-particle excitation peak. Under these circumstances, it seems to be more accurate to compute the quasi-particle peak weight by direct integration of the spectral function around the main peak.

II. THEORY

For convention, we will use atomic units of $e = \hbar = m_e = 1$ throughout this paper unless otherwise indicated. The theory behind these calculations is based on the cumulant expansion outlined in [1, 4]. Namely, that for a core-level XPS, the photo-electron current (which is what is measured in an XPS experiment) may be approximated well by

$$J_k(\omega) = A_c(\omega)$$

where $A_c(\omega)$ is the core-level spectral function, given by

$$A_c(\omega) = \frac{1}{\pi}\mathrm{Im}\int e^{i\omega t}G_c(t)dt \tag{1}$$

where $G_c(t)$ is the core-hole Green's function. The innovation of the cumulant approach [8], as compared with the GWA, is that the core-hole Greens function may be written as

$$G_c(t) = i\theta(t)e^{-i\omega_c t + C(t)} \tag{2}$$

where ω_c is the core-hole energy, $\theta(t)$ is the Heaviside step function, and $C(t)$ is the cumulant (see [4, 6, 8]). This function can be expressed in terms of the neutral quasi-boson excitation spectrum, $\beta(\omega)$ [4], by

$$C(t) = \int_0^\infty \beta(\omega)\left(\frac{e^{i\omega t} - i\omega t - 1}{\omega^2}\right)d\omega \tag{3}$$

Note that $C(t)$ satisfies the following relations:

$$\begin{aligned} &C(-t) = C(t)^* \\ &C(0) = 0 \\ &C'(0) = 0 \end{aligned}$$

Also note that the spectral function is guaranteed to be area-normalized to unity, provided that $C(0) = 0$. To obtain $\beta(\omega)$, we take the Fourier transform of "core-response" function, $\Delta_c(t)$ using the relations[4]

$$\beta(\omega) = \omega\mathrm{Re}\int dt e^{-i\omega t}\Delta_c(t) \tag{4}$$

The core-response function is computed as

$$\Delta_c(t) = \int d^3r V(\vec{r})\delta\rho(\vec{r},t) \tag{5}$$

where $\delta\rho(\vec{r},t)$ is the change in electron density from equilibrium (due to the core-hole perturbation) and $V(\vec{r})$ is the potential due to the presence of the core-hole. This function $\Delta_c(t)$ is computed using RT-TDDFT via a modified version of the SIESTA framework [9]. The details of this simulation procedure will be examined in more depth in the next section; for now, it suffices to know that the function $\Delta_c(t)$ is readily available. It is important to note that since the simulations only involve the valence electron density response, the calculated spectrum only incorporates intrinsic interactions and neglects the interactions with the outgoing core-hole electron (extrinsic interactions).

It is useful to consider the excitation spectrum $\beta(\omega)$ in its own right in addition to the role it plays in computing the spectral function. This is because this spectrum is directly related to the density-density correlation function [4],

$$\chi(\vec{r},\vec{r}\,';\omega) = i\int_0^\infty e^{-i\omega t}\langle\rho(\vec{r},t)\rho(\vec{r}\,',0)\rangle$$

by the relation

$$\beta(\omega) = \int d^3r d^3r' V(\vec{r})V(\vec{r}\,')\mathrm{Im}\ \chi(\vec{r},\vec{r}\,';\omega) \tag{6}$$

In addition to describing the excitation spectrum, it is possible to compute both the quasi-particle peak shift $\Delta E = \omega_{qp} - \omega_c$ and weight Z from $\beta(\omega)$ [3] using the relations

$$\begin{aligned} Z &= \exp\left(-\int_0^\infty \frac{\beta(\omega)}{\omega^2}d\omega\right) \\ \Delta E &= \int_0^\infty \frac{\beta(\omega)}{\omega}d\omega \end{aligned} \tag{7}$$

We will see that these computations, while accurate for the C_{60}, are a bit of an under-estimate in the case of the transition metals. As we will see satellite structures occur without significant gap above the main quasi-particle peak, and this leads to a "blending" of the main quasi-particle peak and the satellite peaks.

III. METHODS

As previously mentioned, the actual calculation of the density response function, $\Delta_c(t)$ was performed using real-time time-dependent density functional theory (RT-TDDFT) via a modified SIESTA fork. This modification, known as RT-SIESTA, uses a real-time, real-space approach and is built up off of the SIESTA ground state DFT package [9]. Time propagation of the density is done using a predictor-corrector Crank-Nicholson operator [4] and densities are expressed using a projection onto a linear combination of localized atomic orbitals. Core electrons are incorporated into the nuclear potentials via the use of pseudo-potentials that are required to have compact support. Since we are approximating the presence of a core-hole in the 1s state, we also neglect any internal structure of the core-hole potential, treating it as a Yukawa potential that is flattened about the origin to avoid any divergences [4]. Typically, the system is relaxed into the ground state electron density using a self-consistency loop. Once it reaches the ground state, the density response is computed by switching on the core-hole potential $V(\vec{r})$, simulating the presence of

a core-hole caused by the ejection of a photoelectron at time $t = 0$. The density is then propagated forward in time and at each time step the core response $\Delta_c(t)$ is measured.

Before using $\Delta_c(t)$ in formula (4), we must subtract off the average value and add in a spectral damping term to render it suitable for the numerical Fourier transform. In addition to the spectral widening applied (typically Gaussian broadening), we also employ a frequency dependent Gaussian widening with variance $\sigma = \frac{1}{\sqrt{2\alpha|\omega|}}$. This widening is meant to replace some of the lost spectral density in the higher energy states due to the use of the localized orbital basis, which cannot replicate the presence of continuum states. Finally, we employ additional broadening terms (typically Lorentzian) when evaluating equation (1) again, to render the functions suitable for numerical Fourier transform.

We also compare the computation of the quasi-particle peak weights by integration of $\beta(\omega)$ with the integration of the XPS spectrum. Specifically, we will compare the theoretically calculated Z value against the calculation of the spectral weight for energies $E > \omega_{qp} + \omega_{\text{threshold}}$. We will use $\omega_{\text{threshold}} = -2\,\text{eV}$. That is, we will compute

$$\tilde{Z}_{\text{threshold}} = \int_{\omega_{\text{threshold}}}^{\infty} A_c(\omega) d\omega \tag{8}$$

where we have shifted $A_c(\omega)$ to peak at ω_{qp}, and compare Z with $\tilde{Z}_{\text{threshold}}$.

IV. RESULTS

A. C_{60} XPS

The experiment we compare out spectral results to is [7]. We first demonstrate some of the steps involved in the calculation of the spectral function. In figure (1) you can see the core response (after subtracting off averages and adding uniform spectral broadening). Note how there is a very large response in the first few fractions of a fs, but this quickly dies off as the system enters equilibrium. After obtaining the core response, we calculate the excitation spectrum density $\beta(\omega)$. As an example, we present β for C_{60} in figure (2). From this, we calculate a quasi-particle peak weight and shift of $Z = .586$ and $\Delta E = 10.7535\,\text{eV}$. Finally, we compute the spectral function. In figure (3) we display the calculated spectral function as well as digitized experimental data from [7]. We have performed a uniform rescaling of the theory to match the data normalization. The agreement in shape between the two is remarkably good, especially for low-energy satellite structures. It appears that at higher energies, the location of the satellite structures is not as accurate. In fact, it appears that the theoretically predicted location of satellite peaks becomes less accurate as energy increases. This could be due to any number of phenomena, including: a lack of extrinsic effects, the use of gaseous fullerene instead of crystalline fullerite, or a byproduct of the simulation techniques. Nevertheless, the agreement is still impressive, certainly justifying our approximation of crystalline fullerite with gaseous fullerene, at least to first order. By employing a numerical peak-finding algorithm the quasi-particle peak shift was found to be $10.7505\,\text{eV}$, in accordance with the result of equation (7). We also found a quasi-particle peak weight by direct integration of $\tilde{Z}_{\text{threshold}} = .573$. This is in good agreement with the theoretically predicted value, as we would expect since there is a clear distinction between the satellite structures and the main peak features. Note that the quasi-particle peak has been shifted by ΔE in all of the plots.

B. Transition Metal XPS

We now turn our attention to the transition metals. We can already tell by looking at the excitation spectra $\beta(\omega)$ in figure (4) that these will have very different spectra from C_{60}. In particular, we note that the metals appear to have a "two-peak" structure whereas C_{60} had a "single-peak" structure. In addition to computing the spectral functions from these, we also use these spectra to compute quasi-particle peak shifts and weights (table I).

Note that in all the spectra in figure (5), the predominant low energy satellite behavior is a broad asymmetric shoulder on the trailing edge of the quasi-particle peak. In the case of Nickel and Iron we can see there is a small, low-energy excitation at around $6\,\text{eV}$ below the main peak. In the case of Cobalt, there is also small low-energy excitation feature, but this occurs at around $12\,\text{eV}$ behind the main peak. All of these spectra appear to exhibit a relatively high degree of asymmetry about their main peak. To see this in more detail, we present a comparison of the "integrated" spectral functions in figure (6). By integrated spectral function we simply mean $I(\omega) = \int_{-\infty}^{\omega} A(\omega')d\omega'$. We also compare these against the fullerene results. Note how the integrated density experiences a rapid increase at the main peak. Simply by visual inspection, it is easy to see that for C_{60} this jump accounts for over 50% of the total spectral weight, in accordance with a Z weight of .58. This is in contrast with the metals, where we can see that the increase due to the main peak is much less pronounced, usually achieving over 50% spectral weight by $-5\,\text{eV}$.

The calculated quasi-particle peak weights and shifts are in table (I), along with the values for fullerene. We also include the computed quasi-particle weight by integration as well as the percent difference between the two (interpreting $\tilde{Z}_{\text{threshold}}$ as the accepted value). The discrepancy for the transition metals should be clear, especially when compared against fullerene. Though in general, we would expect the metallic systems to have low main-peak weights, the numbers calculated by equation (7) are anomalously low. Comparing between fullerene,

which has a clear distinction between satellite peaks and the main peak, we see that the calculation by way of equation (8) and equation (7) only disagree by less than 2%. On the other hand, for metals, it appears that equation (7) can underestimate the quasi-particle weight by over 20%. This discrepancy may be due in part to the numerical procedure used to compute the weights. For finite sample size, lower energy features will inevitably be lost due to a minimum frequency resolution. Thus, for the metallic systems, when the integral for Z is computed, it is possible that these missing low-energy structures are discounted, yielding an underestimate for the quasi-particle energy. This discrepancy may only present itself when these low-energy excitations account for a large amount of spectral weight, as would be the case for these metals. Another explanation is that these computations were not carried out on large enough super-cells and that we are simply seeing residual boundary and edge effects. The investigation of this discrepancy is still an ongoing aspect of this research.

V. SUMMARY AND FUTURE WORK

Via the use of our real-time cumulant based approach, we have have been able to compute the C_{60} core-level XPS with remarkable accuracy. In addition, we compute a quasi-particle peak weight and shift of $Z = .586$ and $\Delta E = 10.75\,\text{eV}$. We also note that the low-energy excitations are reproduced well by this procedure, while the higher energy features are still reproduced, but at incorrect energies. This is likely due to a lack of extrinsic affects as well as neglecting crystalline effects. Overall, the fullerene quasi-particle peak still dominates the spectrum, with almost 60% of the spectral weight. We also have shown that the calculation of Z via equation (7) is in agreement with a direct integration of the XPS spectrum in this case. This is in contrast with the metals, which don't exhibit such a clear distinction between satellite peaks and the main quasi-particle peak. In these cases, we see that the analytic calculation of the quasi-particle peak weight via equation (7) leads to a drastic underestimate of the quasi-particle peak weight, when compared against a direct integration of the spectral function. The exact reason for this discrepancy is still not clear.

Possible directions of future work include simulating crystalline fullerite, determining a more reliable method of computing the spectral weight in the transition metals, increasing the number of unit cells used in the metal calculations, and using these computed spectral functions to compute many-body corrections to calculated single-particle X-Ray Absorption Spectra (XAS).

Sample	Z	$\tilde{Z}_{\text{threshold}}$	%Δ	ΔE
Fe	.316	.397	20.4%	14.433 eV
Co	.283	.437	35.2%	13.873 eV
Ni	.148	.351	57.8%	14.491 eV
C_{60}	.586	.573	1.7%	10.753 eV

TABLE I: Calculated quasi-particle peak weights and shifts for transition metals

VI. ACKNOWLEDGEMENTS

I would like to thank the University of Washington INT REU for making this work possible. In particular, I would like to thank John Rehr, Joshua Kas, and Fernando Vila for all their assistance. Finally, I would like to acknowledge the NSF for helping to support this work.

[1] F. Aryasetiawan, L. Hedin, and K. Karlsson. Multiple plasmon satellites in na and al spectral functions from ab initio cumulant expansion. *Physical Review Letters*, 77(11), 1996.

[2] L. Hedin. New method for calculating the one-particle green's function with application to the electron-gas problem. *Physical Review*, 139(3A), 1965.

[3] L. Hedin. On correlation effects in electron spectroscopies and the gw approximation. *Journal of Physics: Condensed Matter*, 11(R489-R528), 1999.

[4] J.J. Kas, F.D. Vila, J.J. Rehr, and S.A. Chambers. Real-time cumulant approach for charge-transfer satellites in x-ray photoemission spectra. *Physical Review B*, 91(121112(R)), 2015.

[5] H.W. Kroto, J.R. Heath, S.C. O'Brien, R.F. Curl, and R.E. Smalley. C60: Buckminsterfullerene. *Nature*, 318(14), 1985.

[6] D.C. Langreth. Singularities in the x-ray spectra of metals. *Physical Review B*, 1(2), 1970.

[7] J.A. Leiro, M.H. Heinonen, T. Laiho, and I.G. Batirev. Core-level xps spectra of fullerene, highly oriented pyrolitic graphite, and glassy carbon. *Journal of Electron Spectroscopy and Related Phenomena*, 128(205-213), 2003.

[8] P. Nozieres and C.T. De Dominicis. Singularities in the x-ray absorption and emission of metals. iii. one-body theory exact solution. *Physical Review*, 178(3), 1969.

[9] J.M. Soler, E. Artacho, J.D. Gale, A. Garcia, J. Junquera, P. Ordejon, and D. Sanchez-Portal. The siesta method for ab initio order-n materials simulation. *Journal of Physics: Condensed Matter*, 14(2745-2779), 2002.

[10] J. Vinson and J.J. Rehr. Ab initio bethe-saltpeter calculations of the x-ray absoprtion spectra of transition metals at the l-shell edges. *Physical Review B*, 86(195135), 2012.

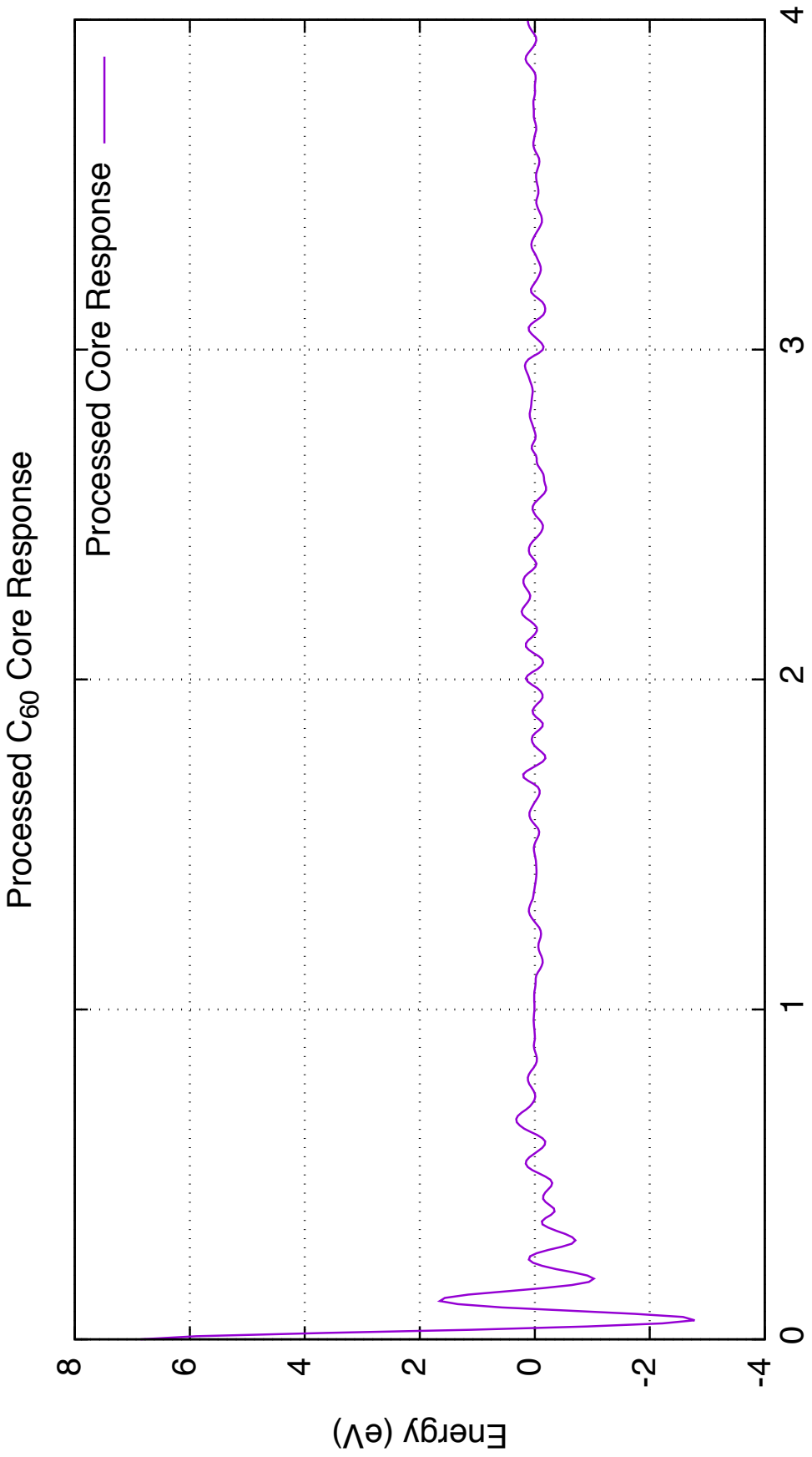

FIG. 1: The processed core response function for C_{60}

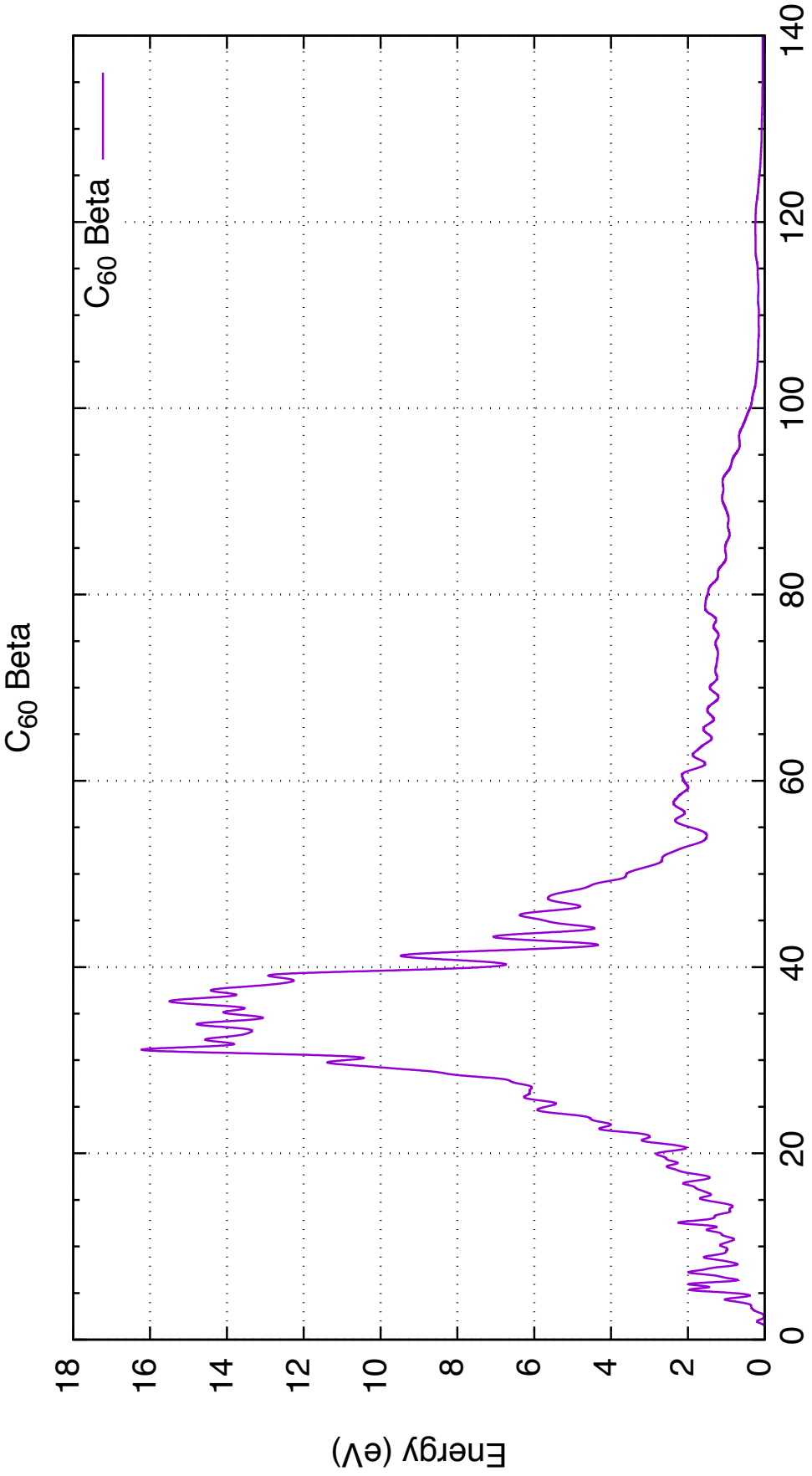

FIG. 2: $\beta(\omega)$ for C_{60}

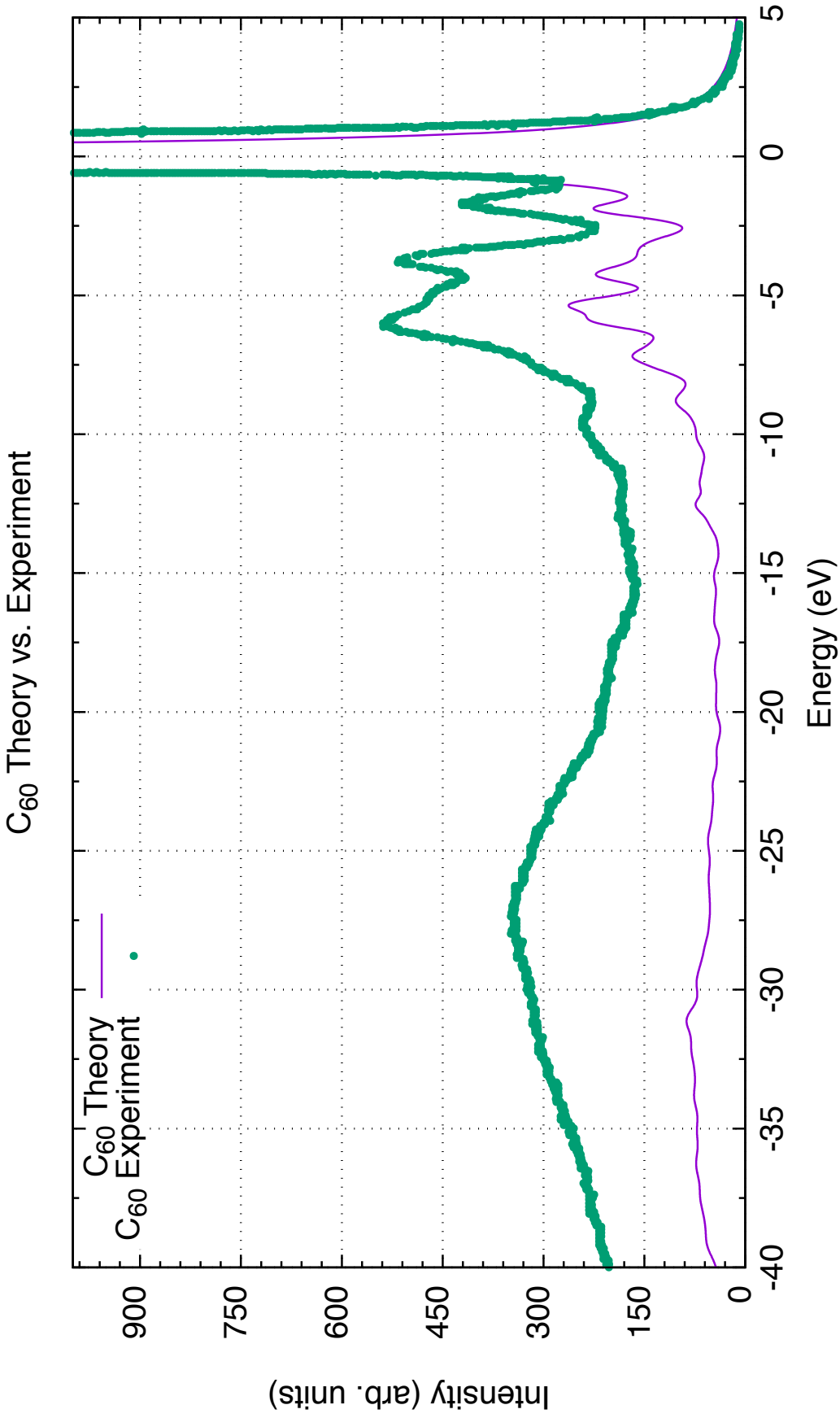

FIG. 3: Comparison of theory and experiment for C_{60} XPS

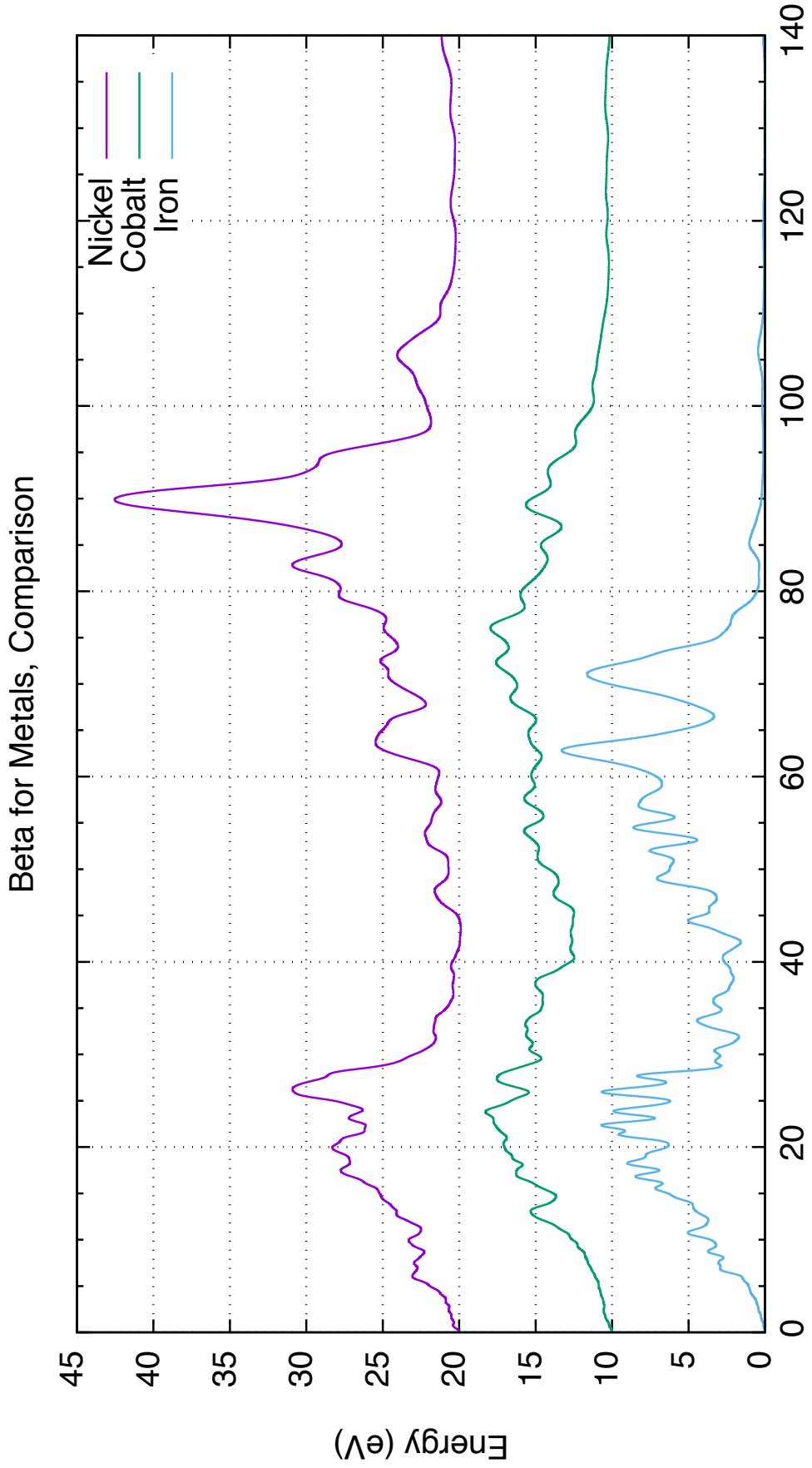

FIG. 4: $\beta(\omega)$ for transition metals. Plots have been shifted vertically for clarity

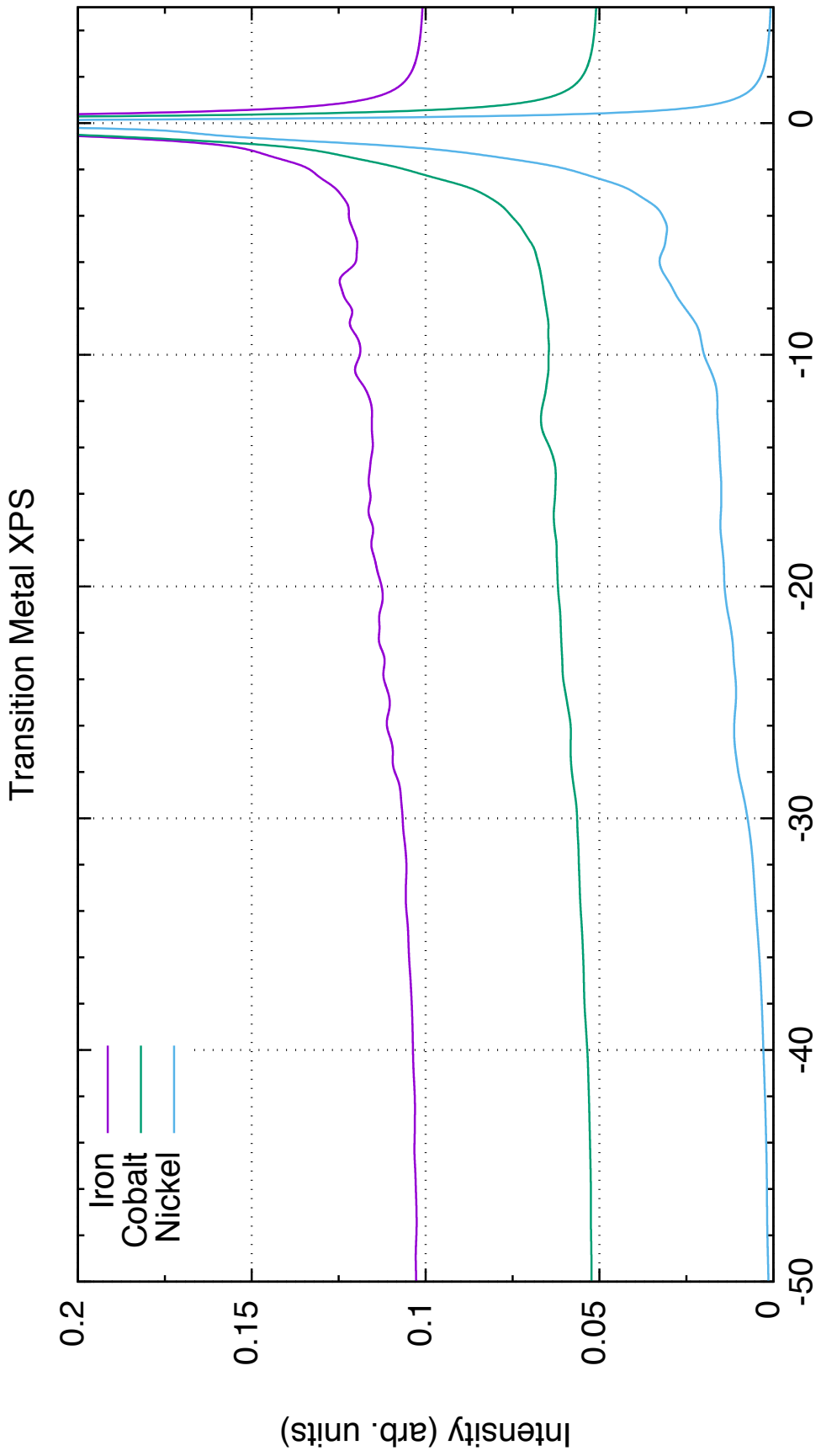

FIG. 5: XPS for transition metals. Spectra have been shifted vertically for clarity

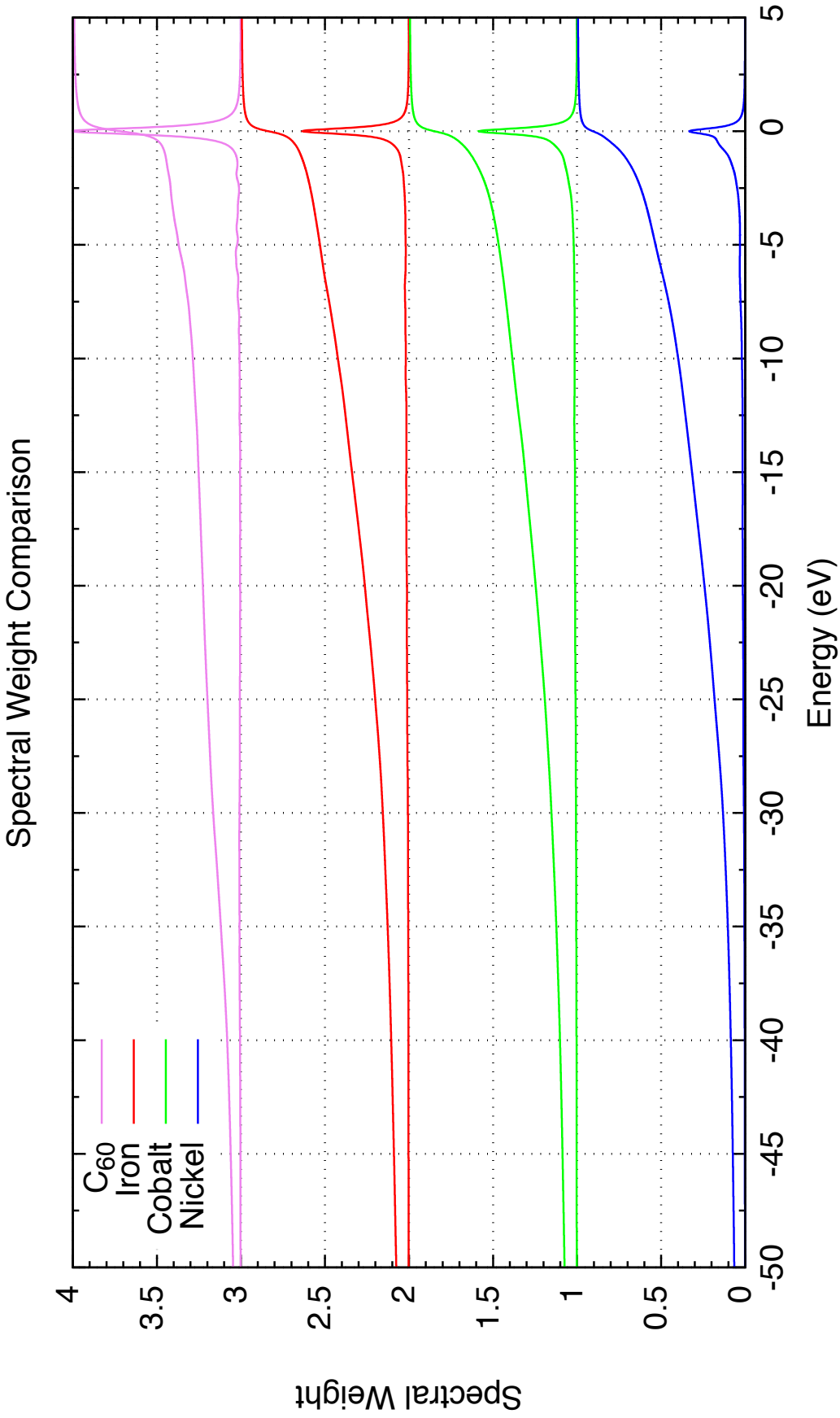

FIG. 6: The spectral functions and integrated spectral functions. Note the vertical shifts for clarity